Diffusion Coefficients Calculated from the Mediterranean Salinity Anomaly in the North Atlantic Ocean[1]

G. T. NEEDLER

Atlantic Oceanographic Laboratory, Bedford Institute of Oceanography, Dartmouth, Nova Scotia, Canada

R. A. HEATH

New Zealand Oceanographic Institute, Wellington, New Zealand

(Manuscript received 28 June 1974, in revised form 12 August 1974)

ABSTRACT

Vertical and horizontal austauch coefficients have been obtained from standard station data on the Mediterranean high-salinity tongue by use of a simple model including advection by a constant velocity and three-dimensional diffusion. It is shown that background effects can be reduced by applying the model to the salinity anomaly relative to a linear θ-S relationship. The analysis gives typical values for K_H of 1.5 to 3×10^7 cm^2 s^{-1} and for K_V of 0.3 to 0.7 cm^2 s^{-1}. It is argued that such values indicate the diffusion of potential density is not important in the main pycnocline of the North Atlantic anticyclonic gyre.

1. Introduction

During the development of physical oceanography, "tongues" of a property have often been used to indicate the flow of one water mass into another. Wüst (1936), for example, used oxygen to describe the flow of North Atlantic deep waters toward the south. Several authors have extended this approach and determined values of austauch coefficients from the change of an oceanic property with position. Defant (1955), for example, used a model for the Mediterranean salinity maximum with advection along the anomaly and horizontal diffusion perpendicular to the axis of the anomaly. More complicated models with diffusion in more than one direction and allowing for velocity shear have been used by other authors, including Warren (1973) who has examined the distribution of several properties in the deep circulation of the South Pacific Ocean.

Somewhat in contrast to inferring the oceanic circulation from its distribution of properties, in recent years a series of theoretical models have evolved which can to some extent describe the distribution of mass in the anticyclonic gyres below the surface frictional layer. A summary of these so called "thermocline" models has been given by Veronis (1969) and more recently by Welander (1971) and Needler (1971). An important feature of the models is that one may fit the general features of the density field in the anticyclonic gyres just as well with models that neglect vertical diffusion of mass as with those that include it in a limited way. The nonlinear nature of the problem has denied either a general solution or any particular solutions including horizontal diffusion of mass.

Even though advective (that is, non-diffusive) models seem to be able to describe the density field in the anticyclonic gyres, changes in temperature and salinity fields which take place along streamlines show that strong diffusive effects are present. One of the most striking examples of such an effect may be seen in the disappearance of the Mediterranean salinity anomaly in one crossing of the North Atlantic. Such a large-scale diffusive feature must make one question the validity of an advective model for the main pycnocline in the North Atlantic. The present work was motivated by the desire to determine whether the advective-diffusive balance in the Mediterranean salinity anomaly implies that there are also significant diffusive effects in the mass balance of the main pycnocline in the North Atlantic. In doing so we are assuming that the diffusion of heat, salt and mass may be described on the large scale by the same austauch coefficients.

In the next sections, the distribution of salt originating from the Mediterranean is discussed and an anomaly suitable for the application of a tongue analysis is derived. From the distribution of this anomaly, we obtain its vertical and horizontal scales, as well as its amplitude, as functions of the distance along the tongue. The vertical and horizontal austauch coefficients are then determined from these quantities using a model of the tongue with three-dimensional diffusion, constant advection, and an initial upstream Gaussian distribution for the anomaly. The results are discussed in the last section and conclusions are drawn as to the im-

[1] Contribution of the Bedford Institute of Oceanography.

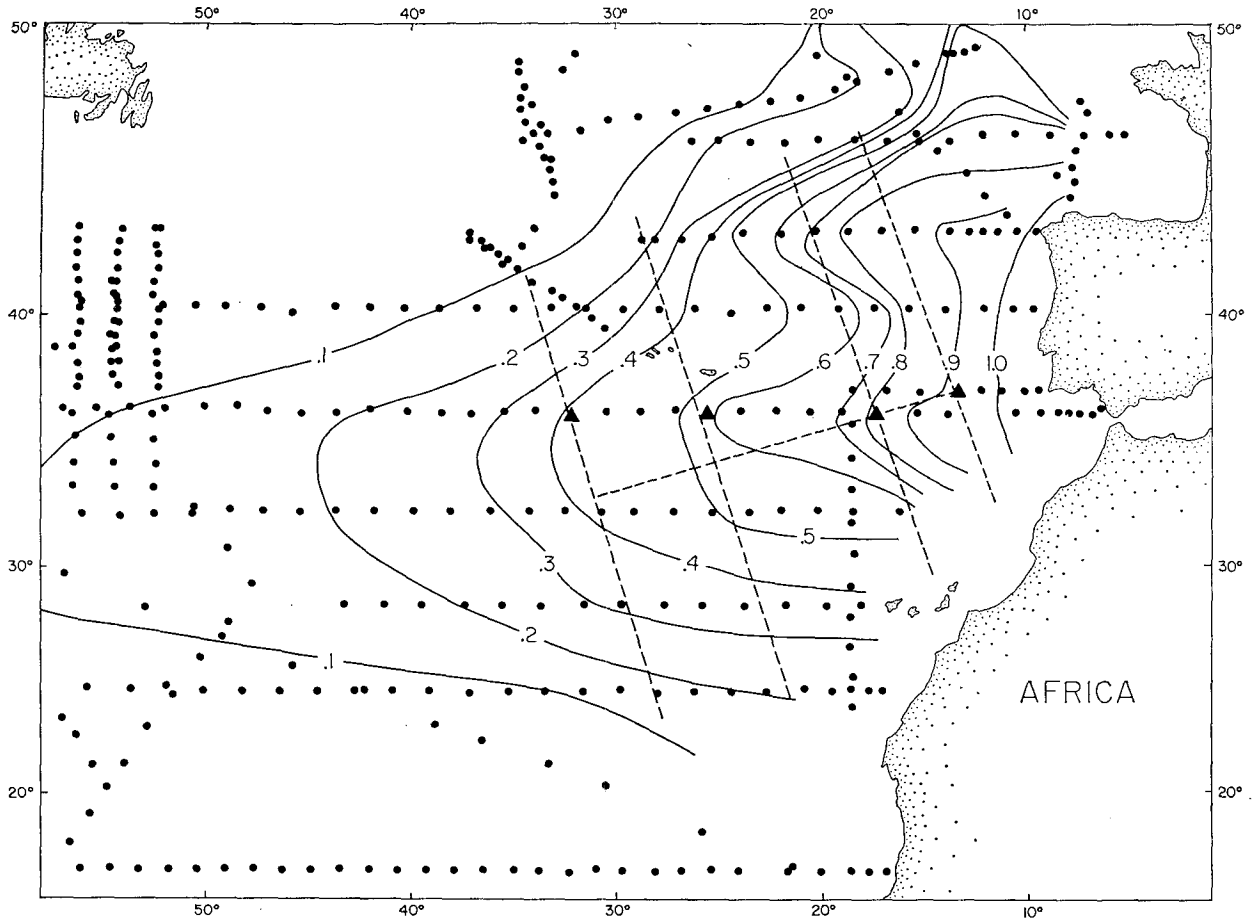

FIG. 1. Salinity anomaly relative to 35.01‰ on the potential density 27.7 surface. The closed circles give the position of the stations, the triangles the position of four particular stations discussed in detail in the text, and the dotted lines the location of four sections discussed in the text and of a line roughly perpendicular to the sections.

portance of diffusion of mass in the large-scale oceanic circulation.

2. The data

The existence of water with comparatively high salinity originating from the Mediterranean has long been known (Sverdrup *et al.*, 1942). One representation of this feature is shown in Fig. 1 which gives the salinity difference from 35.01‰ on the $\sigma_\theta = 27.7$ surface. This surface lies between 1000 and 1200 m over most of the high-salinity region and is at or near the depth of the salinity maximum. The solid circles in Fig. 1 show the positions of a set of oceanographic stations which were selected on the basis of reliable salinities from those stations occupied up to 1969; in the region of high salinity the greatest number of these stations were taken during the IGY. In mid-ocean there are relatively few stations on which to base the contours and even these show considerable scatter about the local mean. On the other hand, it is not difficult to draw through the data points smoothed contours that represent the general trend of the salinity anomaly, which changes by 1‰ over the ocean basin. While part of the smaller scale variance in the salinity anomaly may be due to measurement or interpolation errors, the greatest part no doubt arises from real spatial or temporal differences in the salinity and mass fields. In this paper we will assume that the large-scale diffusive processes may be described by horizontal and vertical austauch coefficients and thus that all the exchanges due to the smaller scale processes may be parameterized and separated from the type of mean as represented by the contours of properties as shown in Fig. 1. The fact one can draw such contours is an indication that a separation of scales exists but whether the diffusion of properties may be represented by use of constant austauch coefficients will only be determined by much better data and more sophisticated analyses than presented here.

The triangles in Fig. 1 give the positions of four stations which lie close to the axis of the tongue and for which the vertical temperature and salinity profiles are shown in Fig. 2. The station numbers increase with distance from the Mediterranean. It may be seen that,

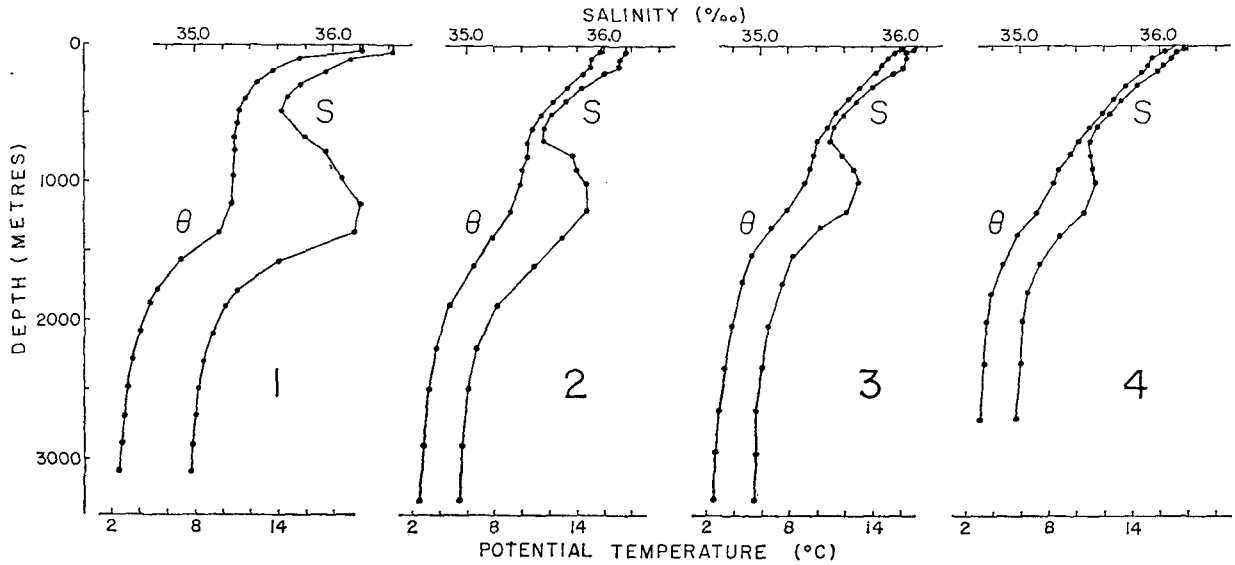

FIG. 2. Potential temperature and salinity profiles for the four stations indicated in Fig. 1. The station number increases with distance from the Mediterranean.

although the vertical sampling interval is sufficient to define the gross shape of the curves, it is not sufficient to resolve all the details. The maximum in salinity at a depth of 1000–1200 m is apparent at all stations although at the fourth station is it receding into the background salinity profile. This is true even though the distance between the mouth of the Mediterranean and the station is only a fraction of the width of the North Atlantic and though the contours given in Fig. 1 are well defined over the whole region. The potential temperature profiles show the compensating change in temperature with depth that is necessary for a monotonic density profile. It may also be noted that the highest salinity water lies at the surface and that the curvature of the profiles is not always the greatest near the maximum. This means that if one wishes to consider the salt balance over a large region while describing the divergence of the vertical diffusion of salt in the usual way by $K_V\partial^2 S/\partial z^2$, one must extend the analysis to regions well away from the subsurface salinity maximum. A way of partially overcoming this problem is given below.

The potential temperature (θ)-salinity (S) relationship for the same four stations is given in Fig. 3. Once again the salinity maximum is clearly present and reasonably well-defined by the available data points. An additional feature which we will make use of is that the θ-S curves not only converge in the deep water, as is to be expected, but also in the upper water at a potential temperature of about 12°C. The dotted line, which may be taken as a hypothetical linear θ-S relationship, passes through the two areas of convergence.

3. The definition of a salinity anomaly

We wish to consider an advective-diffusive balance for the Mediterranean salinity anomaly; that is, a balance described by

$$\mathbf{v}\cdot\nabla S = K_V\frac{\partial^2 S}{\partial z^2} + K_H\nabla_H^2 S, \tag{3.1}$$

where $\mathbf{v}$ is the vector velocity, z the vertical coordinate positive upward, ∇_H^2 the horizontal Laplacian, and K_V, K_H are the vertical and horizontal austauch coeffi-

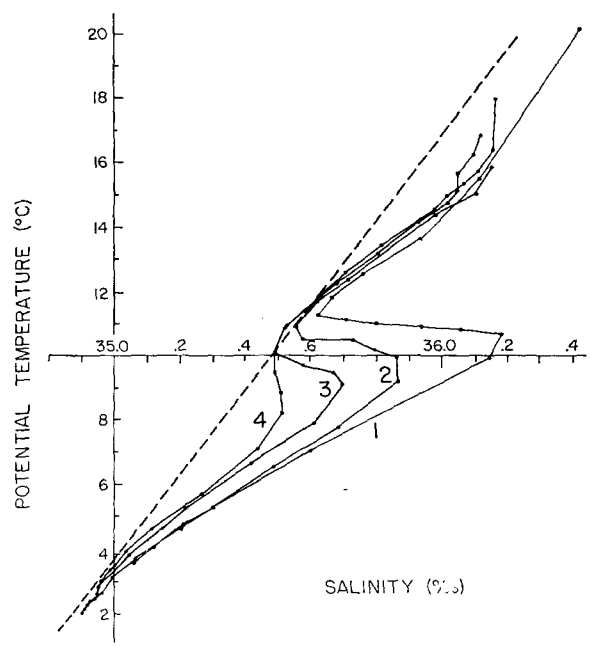

FIG. 3. Potential temperature-salinity curves for the four stations indicated in Fig. 1.

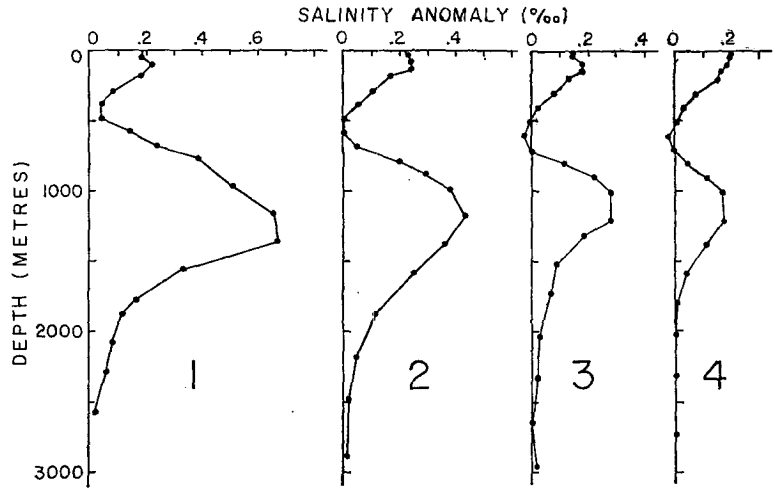

FIG. 4. Salinity anomaly S' for the four stations indicated in Fig. 1.

cients. As long as the diffusion of salt and heat[2] may be parameterized by the same coefficients, we may also write

$$\mathbf{v}\cdot\nabla\theta = K_V\frac{\partial^2\theta}{\partial z^2} + K_H\nabla_H^2\theta. \tag{3.2}$$

Let us now define a salinity anomaly $S'(x,y,z)$ by

$$S(x,y,z) = F[\theta(x,y,z)] + S'(x,y,z), \tag{3.3}$$

where F is an unspecified function of the temperature. It immediately follows upon substituting (3.3) into (3.1) and making use of (3.2) that

$$\mathbf{v}\cdot\nabla S' = K_V\frac{\partial^2 S'}{\partial z^2} + K_H\nabla_H^2 S' + F''\left[K_V\left(\frac{\partial\theta}{\partial z}\right)^2 + K_H\nabla_H\theta\cdot\nabla_H\theta\right], \tag{3.4}$$

where F'' is the second derivative of F with respect to its argument. Clearly if $F''\equiv 0$,

$$\mathbf{v}\cdot\nabla S' = K_V\frac{\partial^2 S'}{\partial z^2} + K_H\nabla_H^2 S', \tag{3.5}$$

and S' satisfies the same advection-diffusion balance as θ and S. If $F''\equiv 0$, one may consider S' as the salinity anomaly relative to a linear θ-S relation[3]; that is, S' is given by

$$S' = S - a\theta - b, \tag{3.6}$$

where a and b are constants. In the remainder of the paper we will work with the anomaly S' where a and b are chosen to give the background linear θ-S relationship shown in Fig. 3.

4. The distribution of the anomaly S'

The vertical profiles of S' for the same four stations as used in Figs. 2 and 3 are given in Fig. 4. Comparison with Fig. 2 shows that, for all the stations, the contribution from the Mediterranean stands out from the background and dominates the effect of the high surface salinity more distinctly using the anomaly S' than S itself. As has been forced by the choice of the linear background θ-S relationship, S' is small around 500–700 m and at large depths. The vertical scale of the anomaly is greater below the maximum than above it for most stations. This may be the result of a greater effective diffusive flux below the maximum as might possibly arise from double-diffusive processes, may reflect the nature of the mixing of the Mediterranean outflow down the continental shelf, or result from the details of the current field. In any event this difference is suppressed in the following analysis.

[2] By taking the diffusion of heat and salt to be described by the same austauch coefficients, we are excluding such processes as salt fingering which can lead to different gross heat and salt fluxes. There is actually strong evidence that salt fingering is an important mechanism underneath the Mediterranean salt anomaly nearer to its origin than the region considered in this paper (Tait and Howe, 1968).

[3] It is worth noting that, if we assume there is a valid θ-S relationship, that is, $S'\equiv 0$ for some function F, then (3.4) requires $F''\equiv 0$. Thus, only a linear θ-S relationship is consistent with the advection-diffusion balance given by (3.1) and (3.2). This is not inconsistent with the usual statement that a linear θ-S relationship arises from the mixing of two discreet water masses. The authors have been unable, however, to find any cases where there are linear θ-S profiles which are strictly independent of position.

Cross-sectional distributions of S' are given in Figs. 5a–d for the four sections shown by the dotted lines in Fig. 1. The sections are numbered in the same sense as the stations they include, that is, the section number increases toward the west. The solid dots indicate the position of the data points used for the contouring. Closely adjacent stations have been used to augment those which fall directly on the sections. One can see that the core of the salinity anomaly is defined by closed isopleths on all four sections. The first two sections are somewhat undefined to the south where they approach the coast of Africa and in the third and fourth sections the vertical scale is most greatly reduced to the north where water of different background θ-S characteristics becomes apparent. In all cases there is a tendency for the vertical scale to increase to the south. Water with a high salinity anomaly S' lies over most of the region and is not plotted. The dotted line in the four sections separates the salinity maximum from the upper region and is defined by where S' becomes negative or passes through a minimum. The four sections of the anomaly S' illustrate a three-dimensional tongue which decreases in amplitude with distance from the Mediterranean.

In the next section we fit the main features of this tongue to a model in which there is three-dimensional diffusion and advection by a constant velocity along the axis of the tongue. Although the use of a constant velocity is a gross approximation, a better velocity field is difficult to obtain. Geostrophic currents calculated from the available stations show considerable variability in magnitude and direction, and depend critically on an unknown reference level. The amount of shear across the anomaly compared to the mean current is also important for any model but can also not be determined without knowledge of a reference level. Much of the variability in the current is no doubt related to similar variability in the salinity anomaly which was noted in the discussion of Fig. 1 and which we have ignored in order to obtain smooth contours. Considering the existence of this relatively small-scale variability and our objective of obtaining large-scale diffusion coefficients, we limit ourselves to applying the model in such a way as to describe the gross changes in the amplitude and vertical and horizontal scales along the axis of the tongue.

The amplitude and the vertical scale of the salinity anomaly have been obtained for each station comprising the four sections by making a least-squares fit to a Gaussian distribution for that part attributed to the Mediterranean outflow. Only those points were used which were at least one-fifth of the maximum value of S' and which were on the same side of any minimum as the tongue. This latter effectively eliminates the higher surface salinity values that may be seen in Fig. 4. The amplitudes obtained in this way for S' in the vertical were then fitted for each section by a Gaussian distribution in the horizontal direction for each of the four sections. The horizontal Gaussian fits are shown in the lower portion of Figs. 5a–d where the arrow indicates the position of the maximum, and the crosses the amplitude for each vertical profile. The amplitudes of the salinity anomaly and its horizontal scales used in the subsequent analysis have been taken from the horizontal Gaussian fits, and the vertical scales from the value obtained by the vertical fit of the station closest to the center of the tongue for each section or, if no single station is at the center, from the average of the most adjacent stations. These values are all given in Table 1.

5. Application of the model to the data

As stated above, we use a model with one-dimensional advection and three-dimensional diffusion, that is, we take

$$K_H\left(\frac{\partial^2 S'}{\partial x^2}+\frac{\partial^2 S'}{\partial y^2}\right)+K_V\frac{\partial^2 S'}{\partial z^2}=u\frac{\partial S'}{\partial x}, \tag{5.1}$$

where x is taken as positive along the center of the tongue, y is the horizontal coordinate across the tongue, z the vertical coordinate, and u the constant velocity in the x direction. The boundary conditions chosen are those which require the anomaly to decay in the downstream direction and satisfy a Gaussian distribution on the surface $x=0$. Thus, we require

$$\left.\begin{aligned} &S'(0,y,z)=S_0'\exp\left(-\frac{y^2}{L^2}-\frac{z^2}{H^2}\right)\\ &S'\to 0 \quad \text{for} \quad x\to+\infty \quad \text{and} \quad y,z\to\pm\infty \end{aligned}\right\}, \tag{5.2}$$

where S_0, L and H will be identified with the observed amplitude and scales of the anomaly S'. It is shown in the Appendix that the solution of (5.1) and (5.2) is given by

$$\begin{aligned} S'(x,y,z)=S_0'\frac{HLu^2}{2K_H(K_HK_V)^{\frac{1}{2}}}\sum_{m=0}^{\infty}\epsilon_m(-1)^m\cos 2m\phi \\ \times\int_0^{\infty}\exp\left[\frac{-k^2u^2}{8}\left(\frac{L^2}{K_H{}^2}+\frac{H^2}{K_HK_V}\right)\right. \\ \left.+\frac{xu}{2K_H}[1-(1+4k^2)^{\frac{1}{2}}]\right]I_m\left[\frac{k^2u^2}{8}\left(\frac{H^2}{K_HK_V}-\frac{L^2}{K_H{}^2}\right)\right] \\ \times J_{2m}\left[ku\left(\frac{z^2}{K_HK_V}+\frac{y^2}{K_H{}^2}\right)^{\frac{1}{2}}\right]dk, \end{aligned} \tag{5.3}$$

where $\epsilon_m=1$ for $m=0$ and $\epsilon_m=2$ for $m\neq 0$ and $\phi=\arctan[z(K_H/K_V)^{\frac{1}{2}}/y]$. It is easily seen that, if $z=y=0$ (that is, on the axis of the tongue) or if $H^2K_H=L^2K_V$, the only contribution to the sum in (5.3)

TABLE 1. Amplitudes and scales for each of the four sections shown in Figs. 1 and 5.

Section	Amplitude A'(‰)	Distance from section 1 (km)	Horizontal scale Y (km)	Vertical scale Z (m)
1	0.646	0	780	500
2	0.450	360	830	470
3	0.260	1070	900	350
4	0.175	1620	1200	400

arises from the $m=0$ term. The latter condition is simply that the ratio of the nondimensional initial scales, $Hu/(K_H K_V)^{\frac{1}{2}}$ and Lu/K_H, is unity. When this is the case, the shape of the nondimensional tongue is independent of x.

If the horizontal austauch coefficient K_H is small enough, then a limit to (5.3) is

$$S'(x,y,z)=\frac{S_0'LH}{[(L^2+4K_Hx/u)(H^2+4K_Vx/u)]^{\frac{1}{2}}} \times\exp\left[-\frac{y^2}{L^2+4K_Hx/u}-\frac{z^2}{H^2+4K_Vx/u}\right], \quad (5.4)$$

which is also the exact solution to (5.1) when the term $K_H\partial^2S'/\partial x^2$ describing diffusive effects along the tongue is neglected. Unfortunately, for the Mediterranean the

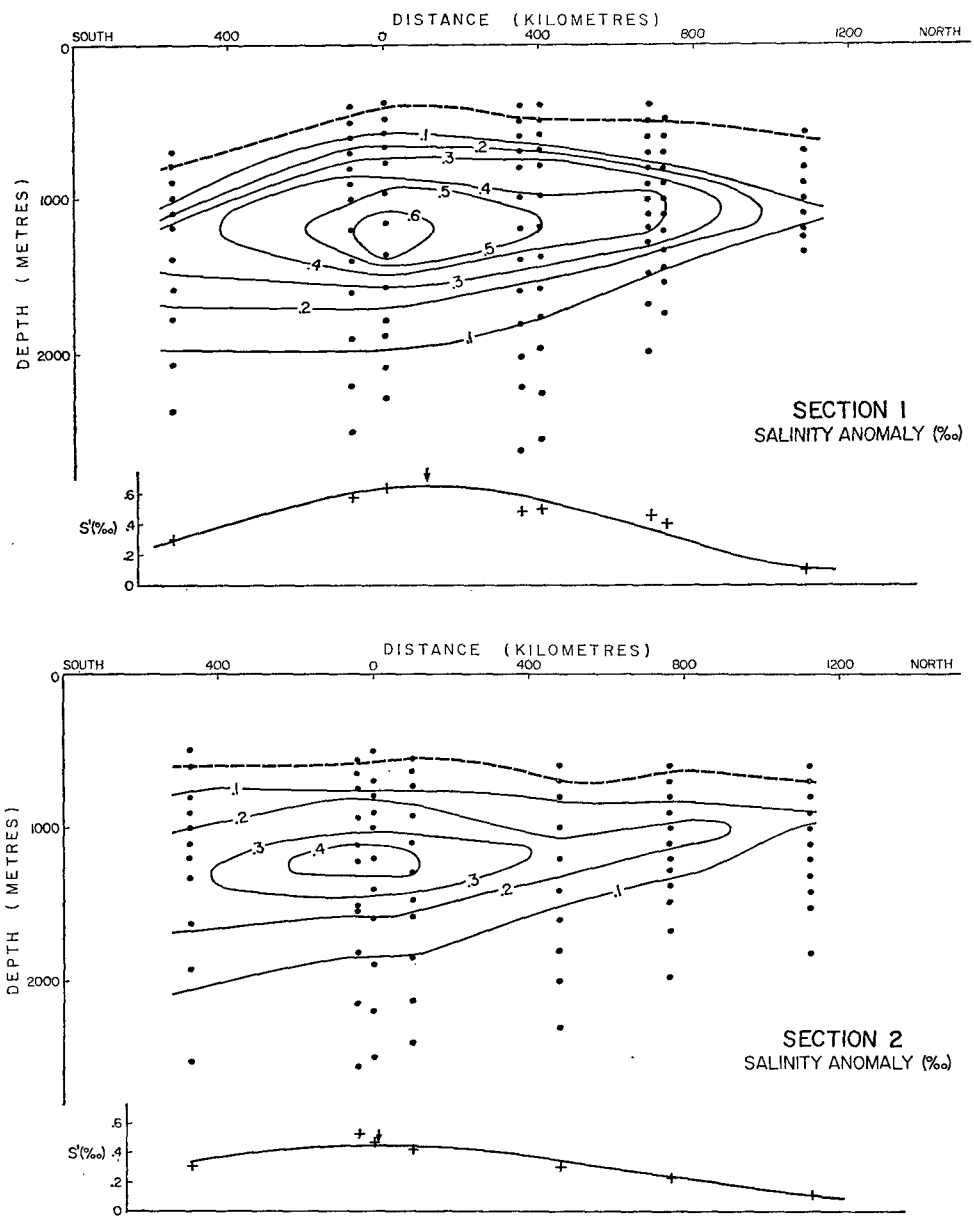

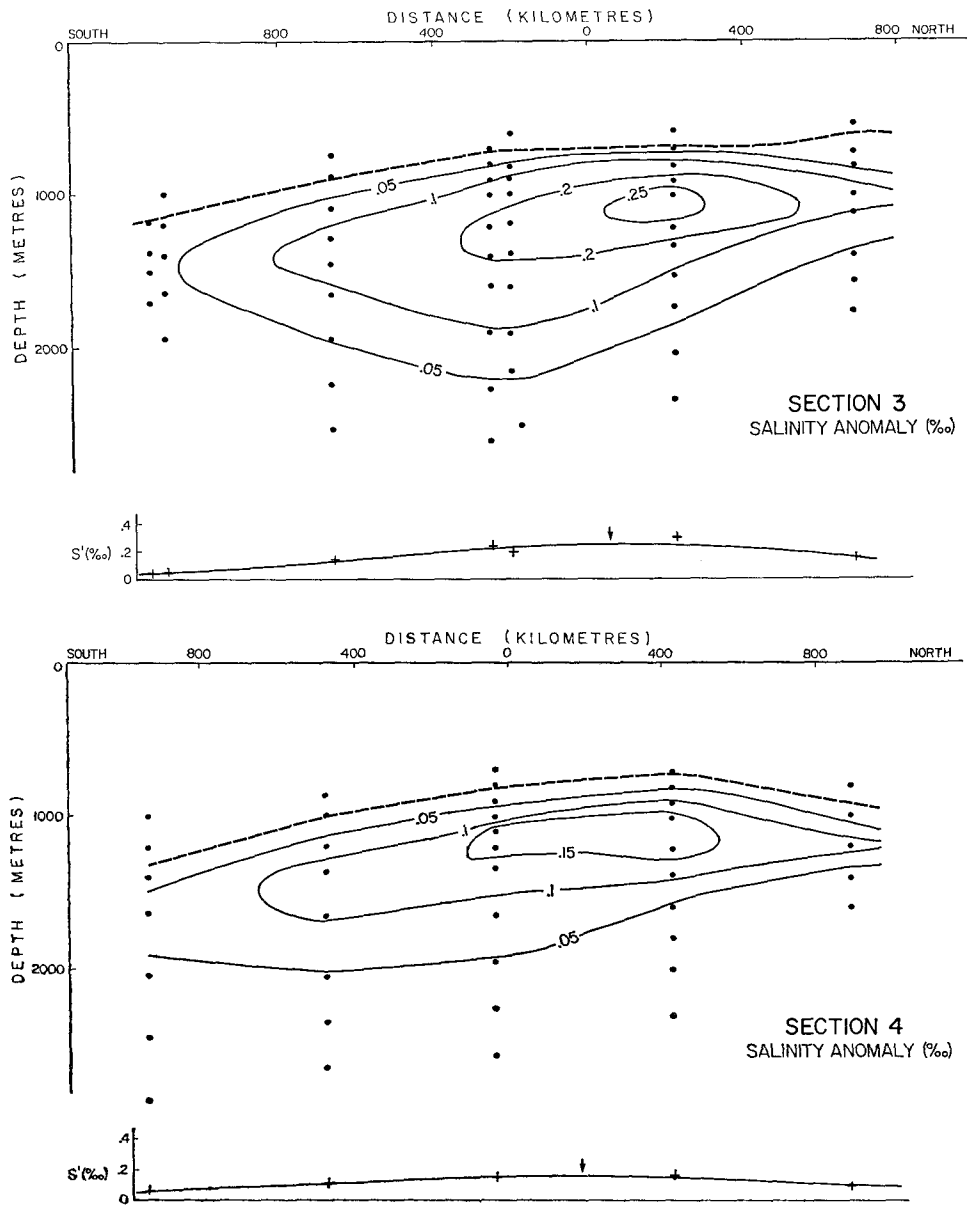

FIG. 5. Salinity anomaly S' for the four sections indicated in Fig. 1. The significance of the dotted lines and the lower graphs is described in the text. The zero in the north-south axis is the position of the intersection of each section with the almost perpendicular line shown in Fig. 1.

diffusion along the tongue has been found in the present work to be important and (5.4) is not a valid approximation. This might be suspected from viewing Fig. 1 since the change in the salinity along the axis of the tongue is similar to that across the tongue. Eq. (5.4) does not in general serve as a valid limit for $K_V=0$ which is given by

$$S'(x,y,z)=\frac{S_0'}{\sqrt{\pi}}\exp(-z^2/H^2)\int_0^\infty \exp\{-(k^2/4)+xu[1-(1+4k^2K_H^2/L^2u^2)^{\frac{1}{2}}/2K_H]\}\times\cos(ky/L)dk. \quad (5.5)$$

It may be shown that (5.5) approaches (5.4) for small enough K_H. One feature of all the solutions, which is easily seen in the approximation (5.4), is that the scales across the tongue increase with distance from the source. This is consistent with diffusion spreading out the initial peaked Gaussian distribution we have chosen and results in the somewhat strange property that the diffusion along the tongue is toward the source if one is far enough removed from the axis. The resulting distribution has a tongue-like character for about one scale length away from the axis and a "tear drop" character at greater distances. In the analysis of the

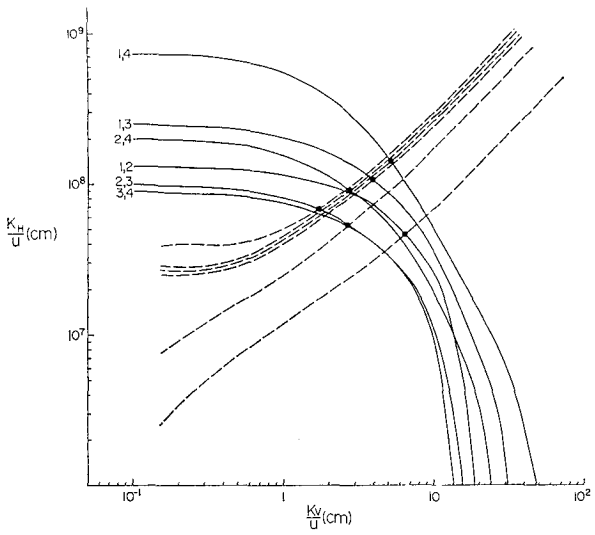

FIG. 6. Vertical and horizontal austauch coefficients obtained from fitting the model to the data. The closed circles at the intersection points of the curves give the best fit values for each pair of sections. The significance of the curves is given in the text.

Mediterranean we are restricted by the data to horizontal distances of about one scale length.

The full solution (5.3) has been used to determine K_H/u and K_V/u from the distribution of the anomaly S'. That only these ratios can be determined, rather than the actual austauch coefficients, can be seen directly from (5.1) or the form of the solution (5.3). The simplest two quantities which can be used to determine K_H/u and K_V/u are the change in the magnitude of the anomaly along the central axis of the tongue and the change in the ratio of the horizontal to vertical scales. The first basically measures the strength of the total diffusion and the second the relative importance of horizontal and vertical diffusion.

The magnitude of the anomaly and its scales were compared to the model for all possible pairs of the four sections described previously. The change in properties are given in Table 2 where the subscripts 0 and 1 indicate the initial and final values respectively. The results are given in Fig. 6. The solid curves show for each pair of sections the possible values of K_H/u and K_V/u for which the model predicts the observed decrease in the magnitude of the anomaly between the sections. For this computation the scales of the upstream section are imposed. The values of K_H/u and K_V/u given by the intersection of the curves with the two axes are in all cases within 1% of the values given by the appropriate asymptotic expressions (5.4) and (5.5). The dotted curves give the possible values of K_H/u and K_V/u for which the anomaly has the same value on the second section one observed scale length away from the axis in both the vertical and horizontal directions. Once again, the upstream scales have been imposed. In this case, the decrease in salinity from one section to the other varies along the curves. The best choice for each pair of sections is indicated by the solid circles which are at the intersection points for each pair of curves.

6. Discussion

Perhaps the most remarkable thing about the results is that the total scatter of values is only from 1.5–6 cm for K_V/u and from 5–15$\times 10^7$ cm for K_H/u. Considering the different oceanic velocities that likely occur over the region, the sparseness of the data, and the general assumptions of the model, this is certainly not large. Several general comments about the results are in order. First, the values of the coefficients are in all cases closer to asymptotic values for strictly horizontal diffusion than for purely vertical diffusion. This is especially true for those pairs of sections not using section 1. This observation coupled with the fact that for most pairs of sections the vertical scale actually decreases along the tongue, instead of increasing, leads one to believe that the diffusive process is principally in the horizontal direction. The finite values for K_V/u that we have obtained may be the result of how we have forced an approximate model to fit the data rather than from any significant amount of vertical diffusion of the anomaly.

A second general property worth noting is that the smallest values of K_H/u arise for the computation involving closest pairs of stations. These may well be the most valid results. The data has been fitted by Gaussian distributions both horizontally and vertically on each section and only those values within one-fifth of the maximum have been used in the vertical. It is perhaps too much to expect that the model would describe the decay of the tongue if the changes are very great or the distances are large enough so that positive or negative anomalies or boundary effects in the far fields can influence the tongue. The values obtained from computations using adjacent pairs of sections come closest to using the model to compute local approximations for the various terms in the equation (5.1). The result for the pair 2, 3 is perhaps the best value obtained because the anomaly is well defined on the two sections and they are far enough away from the coast that the constant velocity condition is not too restrictive. It is probably not coincidental that the value of K_V/u for this case is the smallest obtained.

It was pointed out above that on the average the vertical scale decreases along the tongue. Actually the

TABLE 2. Ratios of the scales and amplitudes for each pair of sections.

Sections	1, 2	1, 3	1, 4	2, 3	2.4	3, 4
L_0H_1/H_0L_1	0.89	0.61	0.52	0.69	0.59	0.80
S_1'/S_0'	0.70	0.40	0.27	0.58	0.39	0.67

only increase is between section 3 and section 4. Some of the non-uniformity in the vertical scale arises from the fact we have forced a Gaussian distribution on profiles such as are shown in Fig. 4. The profiles near the outflow have particularly irregular shapes. In any event, unlike the horizontal scale, the vertical scale does not increase as is required by the model for significant vertical diffusion. As stated above, this is reflected in the values we have obtained for the diffusion coefficients and one might expect that diffusion of the tongue is mainly "horizontal." Actually, as the reader has probably noted, the model has not been applied to a true horizontal since the maxima in the vertical profiles are not at constant depth. A simple analysis shows that the maxima of both S and S' more or less fall along potential density surfaces and more careful analysis shows some tendency for the maxima to cross potential density surfaces as is to be expected considering the magnitude of the salinity anomaly and the nonlinear nature of the equation of state. Because of the problems of interpolating the data and establishing the location of the maxima, no serious attempt has been made to analyze the tongue in terms of mixing across and along density surfaces, even to the extent permitted by ignoring the nonlinearities in the equation of state. The present analysis certainly does not preclude the possibility that the mixing is primarily along density surfaces rather than across them.

In order to obtain the austauch coefficients, one must use a value for the mean velocity u. Such a value is difficult to determine since the value obtained geostrophically is very variable between pairs of stations and because the reference level is not known. If a reference level of 2000–3000 m is used, typical values of u range from 0.2 to 0.4 cm s^{-1}. Using this range of values for u and the results from Sections 2 and 3, one obtains a value for K_H of 1.5 to 3×10^7 cm^2 s^{-1} and for K_V of 0.35 to 0.7 cm^2 s^{-1}. Such values seem to have no significance in the large-scale first-order mass balance in the anticyclonic gyres. Comparing the terms $w\partial\rho^*/\partial z$ and $K_V\partial^2\rho^*/\partial z^2$ in the equation for conservation of potential density ρ^* and using a typical vertical scale of 750 m, one obtains a value for w of -0.5 to -1.0×10^{-5} cm s^{-1}. This velocity is comparable to estimates of deep upwelling velocities but is small compared with the typical downward vertical velocities of 1 to 5×10^{-4} cm s^{-1} below the surface frictional layer that are required to balance the curl of the wind stress. Thus, in the main pycnocline the basic vertical balance must be advective and remain so at least to the depth at which the baroclinic divergence can reduce the surface downward velocity to values of typically 10^{-5} cm s^{-1}. This conclusion is of course not dependent on the present analysis and only depends on having $K_V<1$ cm^2 s^{-1} as is consistent with this model and other analyses such as those involving microstructure (see, for example, Gregg *et al.*, 1973). The effect of horizontal diffusion of ρ^* can be obtained by comparing $K_V\partial^2\rho^*/\partial z^2$ with $K_H\partial^2\rho^*/\partial x^2$. If the ratio K_HH^2/K_VL^2 (where H and L are now typical oceanic vertical and horizontal scales) is not greater than unity, horizontal diffusion is less than vertical diffusion. Taking the values of K_H and K_V given above the ratio is unity for a horizontal scale of about 5000 km, a typically oceanic horizontal scale. Thus, like vertical diffusion, horizontal diffusion for these values of K_H is unimportant in the main pycnocline. If K_V is negligible, the same result can be obtained directly from the comparison of horizontal diffusion terms with the advective terms. The values obtained for K_V and K_H in this paper are unusual in that they have both been obtained from the analysis of one set of data but are typical of many other results in the literature. It is worth noting that the ratio $(K_HH^2)/(K_VL^2)\approx1$ because H/L is also the typical slope of the pycnocline. Thus, it becomes most difficult using the present type of analysis to separate diffusion across and along isopycnals from diffusion in the vertical and horizontal directions since the projection of horizontal processes may appear as diffusion across isopycnals or the diffusion along isopycnals may appear as vertical diffusion. A detailed analysis of θ-S properties on isopycnals can in some cases overcome this problem (see, for example, Pingree, 1972).

Considering the inadequacies of the type of analysis given in this paper, one might ask how better to obtain reasonable estimates of the austauch coefficients from the available oceanographic data on the distribution of properties. The obvious approach is through numerical models but, as pointed out above, the data result in current fields which contain relatively small-scale features. It is difficult to see at present how either to deal with these features directly or to parameterize their effects in a way basically different from that used in this paper unless the model can generate its own mean current field from the basic dynamical equations. This would raise all the problems of dealing with time-dependent processes and detailed topography. Perhaps one might expect advances to come instead from detailed studies of individual processes such as mixing by internal waves, geostrophic eddies, etc.

Acknowledgments. One of the authors (R. A. H.) was supported during most of this work at the Bedford Institute of Oceanography by a National Research Council of Canada post-doctoral fellowship.

APPENDIX

Solution of the Advective-Diffusion Equation

If in Eq. (5.1) we introduce the dimensionless coordinates $x'=ux/K_H$, $y'=uy/K_H$, $z'=uz/(K_HK_V)^{\frac{1}{2}}$, $\Psi=\exp(-x'^{\frac{1}{2}})S'(x',y',z')$, then

$$\nabla'^2\Psi-\tfrac{1}{4}\Psi=0, \tag{A1}$$

where ∇'^2 is the Laplacian operator in the dimensionless coordinates. If we introduce the dimensionless cylindrical coordinates $r=(x'^2+y'^2)^{\frac{1}{2}}$, $\phi=\arctan(z'/y')$, then the solution of (A1) which converges for large r and positive x' is

$$\Psi(r,\theta,x')=J_m(kr)\exp[\pm im\phi-x'(1+4k^2)^{\frac{1}{2}}/2], \quad \text{(A2)}$$

where J_m is the Bessel Function of the first kind of order m. Making use of the Fourier-Bessel integral (Watson, 1962), the general solution satisfying boundary conditions on $x'=0$ may be written as

$$S'(r,\phi,z')=\frac{1}{2\pi}\sum_{\pm m}^{\infty}\int_0^{2\pi}\int_0^{\infty}\int_0^{\infty}S'(r',\phi',0)$$
$$\times\exp\{-im(\phi-\phi')+x'[1-(1+4k^2)^{\frac{1}{2}}]/2\}$$
$$\times J_m(kr')J_m(kr)r'dr'kdkd\phi'. \quad \text{(A3)}$$

Using the value of $S'(r',\phi',0)$ given by (5.2), we may integrate (A3) making use of integral relationships also given in Watson (1962). We obtain

$$S'(r,\phi,x')=\sum_{m=0}^{\infty}\frac{\epsilon_m(-1)^m\cos 2m\phi}{2\alpha\beta}S_0'$$
$$\times\int_0^{\infty}\exp\{-(\alpha^2+\beta^2)k^2/8\alpha^2\beta^2+x'[1-(1+4k^2)^{\frac{1}{2}}]/2\}$$
$$\times I_m[(\alpha^2-\beta^2)k^2/8\alpha^2\beta^2]J_{2m}(kr)kdk, \quad \text{(A4)}$$

where $\alpha=K_H/uL$, $\beta=(K_VK_H)^{\frac{1}{2}}/uH$, $\epsilon_m=1$ for $m=0$ and $\epsilon_m=2$ for $m\neq 0$, and I_m is the modified Bessel function. This is the form of the solution used to obtain (5.3). The two asymptotic solutions (5.4) and (5.5) are easily obtained directly from (A1).

REFERENCES

Defant, A., 1955: Die Ausbreitung des Mittelmeerwassers im Nordatlantischen Ozean. *Pap. Marine Biol. Oceanogr.*, **3**, Suppl., *Deep Sea Res.*, 465–470.

Gregg, M. S., C. S. Cox and P. W. Hacker, 1973: Vertical microstructure measurements in the Central North Pacific. *J. Phys. Oceanogr.*, **3**, 458–69.

Needler, G. T., 1971: Thermocline models with arbitrary barotropic flow. *Deep Sea. Res.*, **18**, 895–903.

Pingree, R. D., 1972: Mixing in the deep stratified ocean. *Deep Sea Res.*, **19**, 549–562.

Sverdrup, H. V., M. W. Johnson and R. H. Fleming, 1942: *The Oceans, Their Physics, Chemistry and General Biology.* Prentice Hall, p. 670.

Tait, R. I., and M. R. Howe, 1968: Some observations of thermohaline stratification in the deep ocean. *Deep Sea Res.*, **15**, 275–80.

Veronis, G., 1969: On theoretical models of thermocline circulation. *Deep Sea Res.*, **16**, Suppl., 301–323.

Warren, B. A., 1973: Transpacific hydrographic sections at latitudes 43S and 28S: The *Scorpio* Expedition—II Deep Water. *Deep Sea Res.*, **20**, 9–38.

Watson, G. N., 1962: *A Treatise on the Theory of Bessel Functions.* Cambridge University Press, 393–395 and 453.

Welander, P., 1971: Some exact solutions to the equation describing an ideal-fluid thermocline. *J. Marine Res.*, **29**, 60–68.

Wüst, G., 1936: Schichtung und Zirkulation des Atlantischen Ozeans. *Meteor-Werk*, Vol. 6, Zeil 1, *Das Bodennanes und die Stratosphäse.*